*36th EPS Conference on Plasma Phys. Sofia, June 29 - July 3, 2009 ECA Vol.**33E**, P-4.138 (2009)*

Plasma Shape Optimization for Steady-State Tokamak Development in DIII-D

C.T. Holcomb[1], J.R. Ferron[2], T.C. Luce[2], T.W. Petrie[2], P.A. Politzer[2], C. Challis[3], J.C. DeBoo[2], E.J. Doyle[4], C.M. Greenfield[2], R.J. Groebner[2], M. Groth[1], A.W. Hyatt[2], G.L. Jackson[2], C. Kessel[5], R.J. La Haye[2], M.A. Makowski[1], G.R. McKee[6], M. Murakami[7], T.H. Osborne[2], J.-M. Park[7], R. Prater[2], G.D. Porter[1], H. Reimerdes[8], T.L. Rhodes[4], M.W. Shafer[6], P.B. Snyder[2], A.D. Turnbull[2] and W.P. West[2]

[1]*Lawrence Livermore National Laboratory, Livermore, California 94551, USA*
[2]*General Atomics, San Diego, California 92186-5608, USA*
[3]*Euratom/UKAEA Fusion Association, Culham Science Centre, Abingdon, OX14 3DB, UK*
[4]*University of California, Los Angeles, California 90095, USA*
[5]*Princeton Plasma Physics Laboratory, Princeton, New Jersey 05843, USA*
[6]*University of Wisconsin, Madison, Wisconsin 53706, USA*
[7]*Oak Ridge National Laboratory, Oak Ridge, Tennessee 37831, USA*
[8]*Columbia University, New York, New York 10027, USA*

I. Introduction

Advanced tokamak research on DIII-D is focused on developing a high fusion gain, steady-state scenario that would eliminate or greatly reduce the demands on an inductive transformer in future devices. Steady-state operation requires the inductively driven current density (j_{Ind}) be zero everywhere. Most of the total current I_p is from self-driven bootstrap current, with the remainder driven by external noninductive sources.

This paper describes an extension of the fully noninductive condition (f_{NI}~100%) to ~0.7 current relaxation times that was achieved by a combination of new scientific insights and more available ECCD. The insights are an optimization of performance through variation of the plasma shape parameter known as squareness (ζ) and an optimization of divertor magnetic balance. These optimizations simultaneously improve stability, confinement, and density control. These are each essential for achieving fully noninductive operation. Bootstrap current fraction f_{BS} is proportional to normalized beta, $\beta_N = \beta_T$ (%)/[I_p (MA)/a(m) B_T (T)], where $\beta_T = 2\mu_0 \langle p \rangle / B_T^2$ is the toroidal beta, a is the equivalent minor radius and B_T the toroidal field. It is desirable to operate at the highest stable β_N with the resulting j_{BS} well aligned with j_{total}. Density control is essential because as density increases, ECCD and neutral beam current drive (NBCD) drive decrease faster than bootstrap current increases. Additional details and relevant references are given in [1].

II. Squareness and Confinement

Optimization of squareness is possible because, unlike elongation and triangularity, squareness adjustments may be made without significantly moving the divertor strike points. Here we limit attention to upper and lower outer ζ, and define it for each with respect to a reference ellipse with semi-major axis at the X-point and semi-minor axis at the low-field side midplane separatrix, as shown in Fig. 1.

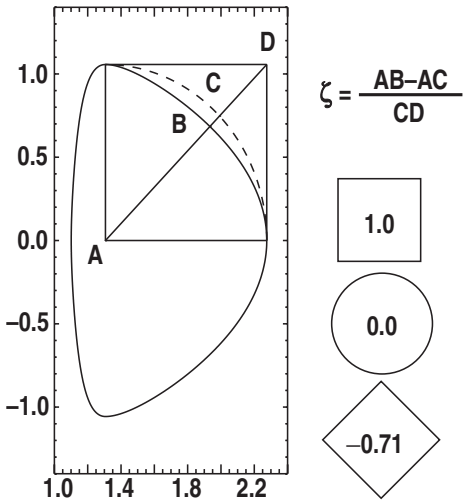

Fig. 1. Squareness (ζ) definition with limiting cases. Dashed line is the reference ellipse.

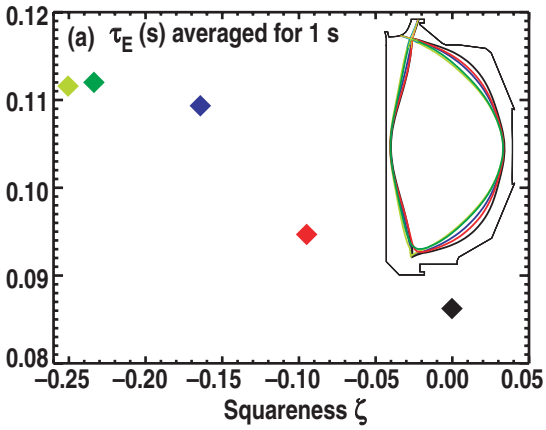

Fig. 2. Energy confinement time at fixed β_N improves with decreasing squareness over the range of the experiment. Inset shows shapes of 5 points produced in DIII-D.

A scan at $\beta_N = 2.4$ shows the global energy confinement time is greatest at the low end of the measured ζ range. A series of double-null discharges ($I_p = 1.1$ MA, $B_T = 1.75$ T, $q_{95} = 5$) was prepared the same way until 2.3 s when ζ was varied to a new value. Injected neutral beam power was feedback controlled to maintain the target β_N in all discharges. Figure 2 shows the energy confinement time τ_E averaged for a 1-s period as a function of ζ calculated from equilibrium reconstructions. A 30% decrease in τ_E is seen as ζ is varied. The confinement trend with ζ persists as β_N is pushed to near the ideal-wall n=1 limit in each case, with the best energy confinement time for the lowest ζ ~70% greater than that for the highest ζ, and $H_{98(y,2)}$ varying from 1.35 to 1.85 [1].

Power balance calculations show increased transport, correlated with measurements of increased turbulence at higher ζ. Figure 3 shows the effective thermal diffusivity profiles for two discharges. The lower ζ discharge ($\zeta \approx -0.25$) has lower thermal transport across most of the profile than the higher ζ discharge ($\zeta \approx 0.0$). This difference is consistent with measurements of low-$k_\perp$ ($\leq 2.5\ \mathrm{cm}^{-1}$) density fluctuations made by a beam emission spectroscopy (BES) diagnostic.

The confinement improvement with decreasing ζ is correlated with a simultaneous increase in pedestal pressure across the range of the experiments. The pedestal pressure profiles prior to an ELM for two discharges with $\zeta = -0.25$ and $\zeta = -0.1$ respectively are compared in Fig. 4 with their shapes in the inset. The lower ζ discharge has ~10% greater pedestal pressure than the higher ζ discharge. This is consistent with a greater pedestal pressure gradient limit for ELM peeling-ballooning stability calculated using the ELITE code with measured profiles as input. Each discharge operates close to the ELM stability limit, but the lower ζ case stability boundary allows access to greater pedestal pressure. The ~19% better confinement time of the low ζ discharge compared to the high ζ is due to reduced transport in both the pedestal and the core.

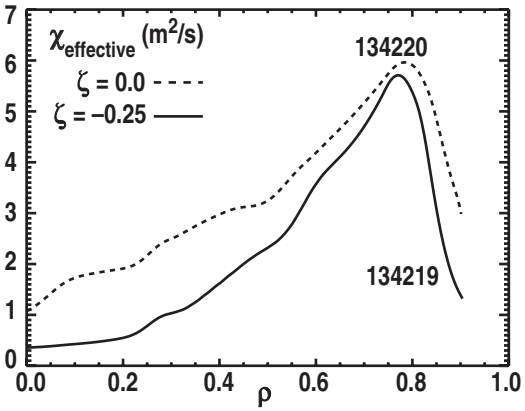

Fig. 3. Effective thermal diffusivity was greater for greater squareness in the range of the experiment.

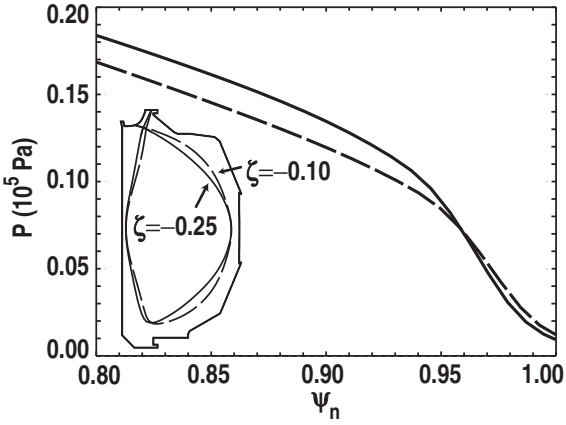

Fig. 4. Achievable pedestal pressure was greater for lower squareness in the range of the experiment.

III. Squareness and Stability

On DIII-D, the experimentally obtained maximum sustainable β_N varies strongly with ζ. This is shown in Fig. 5, where each point represents a different DN discharge. All discharges are formed identically until a ζ change that is completed ~100 ms before a programmed increase in the target β_N. At each ζ, the target β_N was adjusted in successive discharges until the maximum β_N was found that could be sustained for at least a few hundred milliseconds without the occurrence of any large amplitude MHD mode. The maximum achievable β_N was found to occur at intermediate ζ, with ~30% greater β_N than discharges with the highest ζ attempted. Stability modeling predicts the general trend of improved stability with lower ζ.

IV. Density Control Through Divertor Balance Optimization

Magnetic divertor balance has been optimized for density reduction to increase the current from the neutral beam and electron cyclotron systems. This balance is described by $dR_{sep} \equiv$ the radial separation at the low-field side midplane between the flux surfaces connected to the upper and lower divertor X-points. An upper single-null plasma has $dR_{sep}>0$, lower single-null has $dR_{sep}<0$, and magnetically balanced double-null (DN) has $dR_{sep}=0$. Figure 6 shows about a 30% reduction in the line-averaged density is possible using a slightly unbalanced DN, corresponding to dR_{sep} = +0.5 to +1.0 cm. This density reduction depends strongly on whether the ion $\boldsymbol{B}\times\nabla\boldsymbol{B}$ drift points toward or away from the dominant X-point. The reduction is much stronger when the ion $\boldsymbol{B}\times\nabla\boldsymbol{B}$ drift points *away* from the dominant X-point [2].

V. Shape Optimized Fully Noninductive Scenario

These studies identify a moderate squareness shape with a slight divertor bias away from the ion $\boldsymbol{B}\times\nabla\boldsymbol{B}$ drift direction as the optimal for advanced scenario development. Upper and lower outer ζ = –0.13 affords the greatest achievable β_N, with good confinement, and dR_{sep} = 0.5 to 1.0 cm with the ion $\boldsymbol{B}\times\nabla\boldsymbol{B}$ drift directed down maintains a sufficiently low density for auxiliary noninductive current drive.

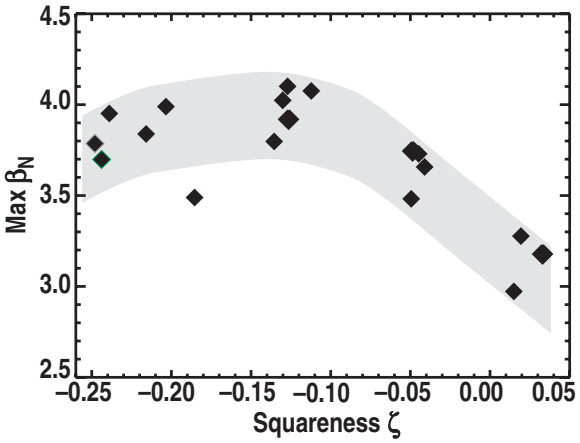

Fig. 5. Maximum sustainable β_N as a function of ζ.

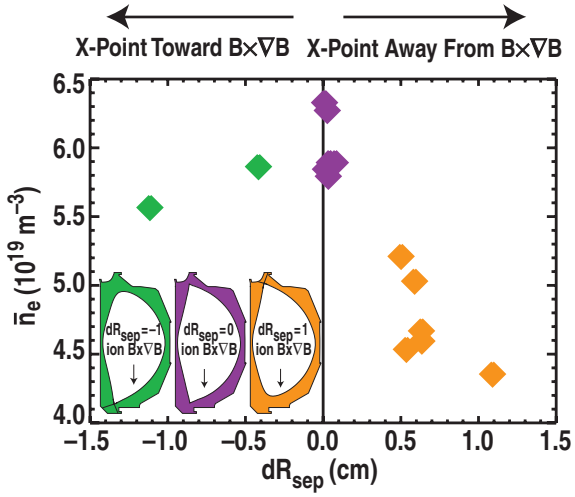

Fig. 6. Density reduction is optimized using a slight divertor bias away from the ion grad(B) drift direction.

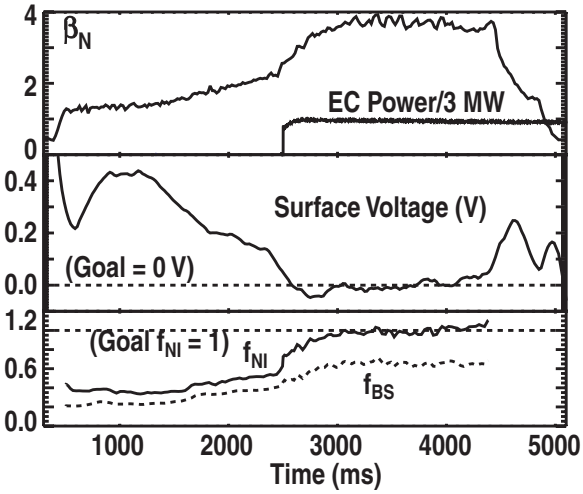

Fig. 7. Shape optimized fully noninductive discharge.

Figure 7 shows the results of one such shape-optimized discharge with B_T = 1.75 T and I_p = 0.9 MA. β_N between 3.5 and 3.9 is sustained for ~2 s without a 2/1 tearing mode, limited only by the available neutral beam energy throughput. q_{min} is about 1.6 and H_{98y2} is about 1.5 at the beginning of this phase. The surface loop voltage is negative or within 10 mV of zero for about 1.7 s, which is about 70% of the current relaxation time. This is a good indication that the inductive current is small during this time. A ONETWO transport code simulation of the current profile evolution indicates f_{NI} near 1 and f_{BS} near 0.65 during the high β phase. β is ~30% above the no-wall limit and approximately at the calculated ideal-wall limit. Further improvements are anticipated with increased off-axis current drive capability and current profile optimization.

This work was performed in part under the auspices of the U.S. Department of Energy by Lawrence Livermore National Laboratory under DE-AC52-07NA27344 and collaborative effort for the US DOE under DE-FC02-04ER54698, DE-FG02-08ER54984, DE-AC02-09CH11466, DE-FG02-89ER53296, DE-AC05-00OR22725 and DE-FG02-89ER53297

References

[1] C.T. Holcomb et al., Phys. Plasmas **16**, 056116 (2009).

[2] T.W. Petrie *et al.*, "Impurity behavior under puff-and pump radiating divertor conditions," accepted for publication in Nucl. Fusion, 2009.